Backstepping Control of an AC/DC/AC Converter in a Grid Connected Wind Power System

YOUSSEF CHAOU[1], SAID ZIANI[2], HAFID BEN ACHOUR[3], ABDELKARIM DAOUDIA[1]
YOUSSEF EL HASSOUANI[3]
[1]OTEA, Department of Physic,
Faculty of Science and Technology Errachidia,
Moulay Ismail University,
BP-509 Boutalamine Errachidia 52 000,
MOROCCO

[2]ENSAM, Mohammed V University in Rabat,
MOROCCO

[3]ENIM, Department of Physic,
Faculty of Science and Technology Errachidia,
Moulay Ismail University,
BP-509 Boutalamine Errachidia 52 000,
MOROCCO

Abstract: - The contribution of this paper is to study a nonlinear control approach known as the backstepping control method to manage reactive and active power using new parametric values for the grid connected wind power generation system. Specifically, the research focuses on a system containing a wind turbine system, a permanent magnet synchronous generator (PMSG), and a grid connected via AC/DC/AC converter. A comprehensive mathematical model for both the wind turbine system, PMSG, and the grid connected via AC/DC/AC converter was developed for this purpose. The Simulation results of the grid-connected wind power generation system are presented and analyzed to show the performance of the nonlinear backstepping control method. The characteristics of the response to variations in generator speed and the power injected into the grid show the highlight of the performance of the backstepping method, under varying wind conditions.

Key-Words: - Nonlinear Control, Backstepping Technique, AC/DC/AC Converter, Wind Power, Turbine-PMSG systems, Reactive and Active Power.

Received: April 16, 2023. Revised: February 13, 2024. Accepted: March 21, 2024. Published: April 26, 2024.

1 Introduction

Wind power is a type of energy that taps into the winds force to generate electricity. It stands as a cost-plentiful energy source that can be captured through wind turbines. These structures are typically installed on structures. Utilize the wind's kinetic energy to create electricity. The wind spins the turbine blades connected to a generator that transforms energy into power. This electrical power can then be utilized to supply energy to households, companies, and neighborhoods. Wind power offers benefits notably being an eco-renewable energy option. It doesn't emit air pollutants or greenhouse gases playing a role, in reducing our reliance, on fuels, [1]. Furthermore, the price of wind power is getting more competitive compared to energy sources, which is drawing interest, from communities and businesses. In general wind power can significantly contribute to the shift, towards a dependable energy infrastructure. Presently the primary generators utilized in wind power generation include the fed generator and the permanent magnet synchronous generator, [2]. Faced with the problems of wind and water power production, the permanent magnet synchronous generator has advantages such as no excitation circuit, and low maintenance. Thanks to these advantages, the use of the permanent magnet synchronous generator makes the variable speed wind power conversion systems more attractive than the fixed speed ones because of the possibility of extracting the optimal energy in different operating

conditions. In this paper, the authors propose a modeling study and behavioral simulations of a wind power generation system based on a permanent magnet synchronous machine connected to the grid by an AC/DC/AC converter, [3]. In a wind power system connected to the grid, the AC/DC/AC converter plays a role, in converting and transmitting power. Its effectiveness directly impacts the performance of the wind power setup. To transfer the captured wind energy back to the grid the three phases produced by the machine with varying frequency and amplitude are rectified using a back-to-back converter (AC/DC/AC). The AC side connects, to the stator of PMSG while the converter output (DC/AC) links directly to the grid through a coil. This setup offers benefits. While traditional PI controllers can manage this system they may not always ensure performance in terms of stability and disturbance control, [4], [5]. To address this issue different advanced control techniques have been suggested for managing and overseeing the wind power generation setup, including input-output linearization control, [6], sliding mode control [7], backstepping control, [8], [9], [10], [11] and DTC. Backstepping has emerged as a promising alternative approach for controlling nonlinear systems. It integrates the selection of Lyapunov functions with control laws, enabling the maintenance of global system stability at all times, [12].

2 Modeling of the Systems Elements

2.1 Model of the Turbine and the Permanent Magnet Synchronous Machine

The theoretical power delivered to the turbine can be represented by equation (1), where ρ denotes the density of air, S represents the circular area swept by the turbine blades, β is the pitch angle of the blades, and V indicates the velocity of the wind in meters per second (m/s).

$$P_t = \frac{1}{2}\ C_p(\lambda,\beta).\rho.S.V^3 \quad (1)$$

The ratio of turbine speed to wind speed is expressed by (2), where Ω_t is the rotational speed of the turbine, R_t is the blade radius.

$$\lambda = \frac{\Omega_t.R_t}{V} \quad (2)$$

The power coefficient (C_p) has a theoretical limit of 0.59 called the "Betz limit". This limit is never reached in practice. This coefficient can be estimated using (3).

$$C_p(\lambda,\beta) = A_1\left[\left(\left(\frac{A_2}{\lambda_i}\right) - A_3\beta - A_4\right)e^{\frac{A_5}{\lambda_i}} + A_6\lambda\right] \quad (3)$$

With: $\frac{1}{\lambda_i} = \frac{1}{\lambda+0.08.\beta} - \frac{0.035}{\beta^3+1}$, $A_1 = 0.5$, $A_2 = 116$, $A_3 = 0.4$, $A_4 = 5$, $A_5 = -21$ and $A_6 = 0.0068$

The mechanical torque of the wind turbine $C_g$obtained from the mechanical power is expressed by (4).

$$C_g = \frac{P_t}{\Omega_t} \quad (4)$$

The mechanical equation of the system is expressed by (5), where J_t and J_g have the moments of inertia of the turbine and the generator, respectively, f_t and f_g have the coefficients of the viscous friction of the turbine and the generator, respectively, Ω_{mec} is the rotational speed of the generator, and G the speed multiplier ratio.

$$C_g - C_{em} = J\frac{d\Omega_{mec}}{dt} + f\Omega_{mec} \quad (5)$$

With: $J = J_g + \frac{J_t}{G^2}$ et $f = f_g + \frac{f_t}{G^2}$

The electrical model of an PMSM in generator operation is reproduced from the model of the machine in motor operation model of the machine in motor operation, by reversing the direction of the currents i_d and i_q in the Park marks. The model of the permanent magnet synchronous generator PMSG thus obtained can be written in the following form (6):

$$\begin{cases} \frac{di_d}{dt} = -\frac{R_s}{L_d}i_d + \frac{L_q}{L_d}\omega i_q - \frac{1}{L_d}v_d \\ \frac{di_q}{dt} = -\frac{R_s}{L_q}i_q - \frac{L_d}{L_q}\omega i_d + \frac{\varphi_f}{L_q}\omega - \frac{1}{L_q}v_q \\ \frac{d\Omega}{dt} = -\frac{P}{J}i_q[(L_d - L_q)i_d + \varphi_f] - \frac{f}{J}\Omega + \frac{1}{J}C_g \end{cases} \quad (6)$$

Note that $\Omega = \Omega_{mec}$ for driving a PMSG by the wind turbine where R_s is the stator resistance, L_d and L_q are the inductances in the (d, q) frame, i_d and i_q are the stator currents, ω is the electrical velocity of the and φ_f is the PMSG remanent flux.

2.2 Model of the Converters and the Electric Grid

The system has a static AC/DC/AC converter with the rectifier on the machine side and the inverter on the grid side. The model of AC/DC/AC converter is given by (7), where C is the DC bus capacitance, I_{dc} is the rectifier current and I_{inv} is the inverter current.

$$C\frac{dV_{dc}}{dt} = I_{dc} - I_{inv} \tag{7}$$

The inverter model is presented by (8), where V_{sa}, V_{sb} and V_{sc} are the three-phase voltages at the output of the inverter and V_{dc} is the DC bus voltage.

$$\begin{bmatrix} V_{sa} \\ V_{sb} \\ V_{sc} \end{bmatrix} = \frac{V_{dc}}{3}\begin{bmatrix} 2 & -1 & -1 \\ -1 & 2 & -1 \\ -1 & -1 & 2 \end{bmatrix}\begin{bmatrix} S_a \\ S_b \\ S_c \end{bmatrix} \tag{8}$$

The analytical model of the power system is presented by (9), where V_{gd} and $V_{gq}$are the electromotive force of the system in the park reference (d, q), R_g and L_g are the resistance and inductance of the lines.

$$\begin{cases} \frac{di_{gd}}{dt} = -\frac{R_g}{L_g}i_{gd} - \omega i_{gq} + \frac{1}{L_g}E_d - \frac{1}{L_g}V_{gd} \\ \frac{di_{gq}}{dt} = -\frac{R_g}{L_g}i_{gq} + \omega i_{gd} + \frac{1}{L_g}E_q - \frac{1}{L_g}V_{gq} \end{cases} \tag{9}$$

Whith: $E_d = S_{gd}V_{dc}$ and $E_q = S_{gq}V_{dc}$

In addition, the active and reactive power expressions can be calculated according to the following equations:

$$\begin{cases} P = V_{gd}i_{gd} + V_{gq}i_{gq} \\ Q = V_{gq}i_{gd} - V_{gd}i_{gq} \end{cases} \tag{10}$$

3 System Control Studied by Backstepping Technique

The equation (11) is the model of the global system studied in the park reference (d, q) it can be written as:

$$\begin{cases} \frac{di_d}{dt} = -\frac{R_s}{L_d}i_d + \frac{L_q}{L_d}\omega i_q - \frac{1}{L_d}v_d \\ \frac{di_q}{dt} = -\frac{R_s}{L_q}i_q - \frac{L_d}{L_q}\omega i_d + \frac{\varphi_f}{L_q}\omega - \frac{1}{L_q}v_q \\ \frac{d\Omega}{dt} = -\frac{P}{J}i_q[(L_d - L_q)i_d + \varphi_f] - \frac{f}{J}\Omega + \frac{1}{J}C_g \\ \frac{dV_{dc}}{dt} = \frac{I_{dc}}{C} - \frac{V_{gd}i_{gd} + V_{gq}i_{gq}}{CV_{dc}} \\ \frac{di_{gd}}{dt} = -\frac{R_g}{L_g}i_{gd} + \omega i_{gq} + \frac{1}{L_g}E_d - \frac{1}{L_g}V_{gd} \\ \frac{di_{gq}}{dt} = -\frac{R_g}{L_g}i_{gq} - \omega i_{gd} + \frac{1}{L_g}E_q - \frac{1}{L_g}V_{gq} \end{cases} \tag{11}$$

The equation (11) represents the dynamic model of a nonlinear system whose general form (12) is the following:

$$\dot{X} = F(X) + G(X)U \tag{12}$$

4 Backstepping Control Design

The backstepping controller is considered a very useful tool when some states are controlled by other states. This technique uses one state as a virtual controller to another state since the system is in triangular feedback form. It also overcomes the problem of finding a Lyapunov control function as a design tool. The design of backstepping control, nonlinear systems or subsystems of the form (13).

$$\begin{gathered} \dot{x}_1 = f_1(x_1) + g_0(x_1)x_2 \\ \dot{x}_2 = f_2(x_1, x_2) + g_1(x_1, x_2)x_3 \\ \vdots \\ \dot{x}_n = f_n(x_1, \ldots, x_n) + g_{n-1}(x_1, \ldots, x_n)u \end{gathered} \tag{13}$$

Where: $x = [x_1, x_2, \ldots, x_n]^T \in \Re^n$, $u \in \Re$

We wish to make the output $y = x$ follow the reference signal y_{ref} supposed to be known. The system being of order n, the design is done in n steps.

5 Designed of Backstepping Controller

The application of this approach on the permanent magnet synchronous generator allows us to determine the constituents of the control voltages of the machine, by ensuring the machine, ensuring the global stability by the Lyapunov theory.

The errors defined by the expressions:

$$\begin{cases} e_1 = i_{dref} - i_d \\ e_2 = \Omega_{ref} - \Omega \\ e_3 = i_{qref} - i_q \\ e_4 = V_{dcref} - V_{dc} \\ e_5 = i_{gdref} - i_{gd} \\ e_6 = i_{gqref} - i_{gq} \end{cases} \tag{14}$$

The errors dynamics is given by:

$$\begin{cases} \dot{e}_1 = \dot{i}_{dref} - \dot{i}_d \\ \dot{e}_2 = \dot{\Omega}_{ref} - \dot{\Omega} \\ \dot{e}_3 = \dot{i}_{qref} - \dot{i}_q \\ \dot{e}_4 = \dot{V}_{dcref} - \dot{V}_{dc} \\ \dot{e}_5 = \dot{i}_{gdref} - \dot{i}_{gd} \\ \dot{e}_6 = \dot{i}_{gqref} - \dot{i}_{gq} \end{cases} \tag{15}$$

5.1 Step 1: Control of i_d

The current i_d of the PMSG is always forced to be zero, so the d-axis flux is zero and all coupling flux is directed along the q-axis to obtain maximum electromagnetic torque. To ensure the control of the current i_d, we adopt the following "Lyaponov" function:

$$V_1 = \frac{1}{2}e_1^2 \quad (16)$$

Making a derivative of this function (16), we will have:

$$\dot{V}_1 = e_1\dot{e}_1$$
$$\dot{V}_1 = e_1(\dot{i}_{dref} - \dot{i}_d) \quad (17)$$

We choose:

$$\dot{e}_1 = -K_1e_1 = \dot{i}_{dref} + \frac{R_s}{L_d}i_d - \frac{L_q}{L_d}\omega i_q + \frac{1}{L_d}v_d \quad (18)$$

Where K_1 is a positive scalar.
Then $\dot{V}_1 = -K_1e_1^2 \leq 0$ and the backstepping control law v_{dref} is designed as:

$$v_{dref} = L_d[-K_1e_1 - i_{dref} - \frac{R_s}{L_d}i_d + \frac{\omega L_q}{L_d}i_q] \quad (19)$$

5.2 Step 2: Control of Rotor Speed

As the rotor speed is the main control variable, its trajectory is defined as the reference value and the control error as:

$$\dot{e}_2 = \dot{\Omega}_{ref} + \frac{P}{J}i_q[(L_d - L_q)i_d + \varphi_f] + \frac{f}{J}\Omega - \frac{1}{J}C_g \quad (20)$$

Define the second Lyapunov function as:

$$V_2 = V_1 + \frac{1}{2}e_2^2 \quad (21)$$

And

$$\dot{V}_2 = \dot{V}_1 + e_2\dot{e}_2 = -K_1e_1^2 + e_2\dot{e}_2 \quad (22)$$

In order to obtain $\dot{V}_2 \leq 0$, we can choose:

$$\dot{e}_2 = -K_2e_2 \quad (23)$$

Where K_2 is a positive scalar
Then

$$-k_2e_2 = \dot{\Omega}_{ref} + \frac{P}{J}i_q[(L_d - L_q)i_d + \varphi_f] + \frac{f}{J}\Omega - \frac{1}{J}C_g$$
$$i_{qref} = (-\dot{\Omega}_{ref} - k_2e_2 - \frac{f}{J}\Omega + \frac{1}{J}C_r)\frac{J}{P[(L_d - L_q)i_d + \varphi_f]} \quad (24)$$

Considering that $i_{dref} = 0$ this leads to defining i_{qref} the command necessary to determine the v_{qref} voltage.

$$i_{qref} = (-k_2e_2 - \dot{\omega}_{dref} - \frac{f}{J}\omega + \frac{1}{J}C_r)(\frac{J}{P\varphi_f}) \quad (25)$$

5.3 Step 3: Control of i_q

In the following, the assurance of stability and convergence of the i_q component to the reference i_{qref}, leads us to choose the following "Lyapunov" function:

$$V_3 = V_1 + V_2 + \frac{1}{2}e_3^2 \quad (26)$$

Then $\dot{V}_3 = -K_1e_1^2 - K_2e_2^2 + e_3\dot{e}_3$

To obtain $\dot{V}_3 \leq 0$, we can choose

$$\dot{e}_3 = -K_3e_3 \quad (27)$$

Where K_3 is a positive scalar

$$\dot{V}_3 = \dot{V}_1 + \dot{V}_2 + e_3\dot{e}_3$$
$$\dot{e}_3 = -K_3e_3 = \dot{i}_{qref} + \frac{R_s}{L_q}i_q - P\frac{L_d}{L_q}\Omega\, i_d + P\frac{\varphi_f}{L_q}\Omega - \frac{1}{L_q}v_q \quad (28)$$

We deduce v_{qref} the final backstepping control law is designed as:

$$v_{qref} = L_q[K_3e_3 + \dot{i}_{qref} + \frac{R_s}{L_q}i_q + \frac{P\Omega}{L_q}(L_di_d + \varphi_f)] \quad (29)$$

5.4 Step 4: Control of V_{dc}

In the following, the assurance of stability and convergence of the V_{dc} component to the reference V_{dcref}, leads us to choose the following "Lyaponov" function:

$$V_4 = \frac{1}{2}e_4^2 \quad (30)$$

Making a derivative of this function (30), we will have:

$$\dot{V}_4 = e_4\dot{e}_4$$
$$\dot{V}_4 = e_4(\dot{V}_{dcref} - \dot{V}_{dc}) \quad (31)$$

We choose:

$$\dot{e}_4 = -K_4e_4 = \dot{V}_{dcref} + \frac{V_{gd}i_{gd} + V_{gq}i_{gq}}{CV_{dc}} - \frac{I_{dc}}{C} \quad (32)$$

Where K_4 is a positive scalar
Then $\dot{V}_4 = -K_4e_4^2 \leq 0$ and the backstepping control law i_{gdref} is designed as:

$$i_{gdref} = \frac{1}{V_{gd}}(-K_4CV_{dc}e_4 + V_{dc}I_{dc} - V_{gq}i_{gq}) \quad (33)$$

5.5 Step 5: Control of i_{gd}

In the following, the assurance of stability and convergence of the i_{gd} component to the reference i_{gdref}, leads us to choose the following "Lyaponov" function:
Define the second Lyapunov function as:

$$V_5 = V_4 + \frac{1}{2}e_5^2 \quad (34)$$

And $\dot{V}_5 = \dot{V}_4 + e_5\dot{e}_5 = -K_4e_4^2 + e_5\dot{e}_5$ (35)

To obtain $\dot{V}_5 \leq 0$, we can choose

$$\dot{e}_5 = -K_5e_5 \quad (36)$$

Where K_5 is a positive scalar
Then

$$-k_5e_5 = \frac{R_g}{L_g}i_{gd} - \omega i_{gq} - \frac{1}{L_g}E_d + \frac{1}{L_g}V_{gd} \quad (37)$$

The backstepping control law E_{dref} is designed as:

$$E_{dref} = L_g(k_5 e_5 + \frac{R_g}{L_g} i_{gd} - \omega i_{gq} + \frac{1}{L_g} V_{gd} + i_{gdref}) \quad (38)$$

5.6 Step 6: Control of i_{gq}

The reactive power is always forced to be zero (Q=0), to ensure the quality of the energy injected into the electrical network and also to determine the reference current i_{gqref}. In view of ensuring the control of the current i_{gq}, we adopt the following "Lyaponov" function:

$$V_6 = V_4 + V_5 + \frac{1}{2} e_6^2 \quad (39)$$

Then $\dot{V}_6 = -K_4 e_4^2 - K_5 e_5^2 + e_6 \dot{e}_6$

To obtain $\dot{V}_6 \leq 0$, we can choose:

$$\dot{e}_6 = -K_6 e_6 \quad (40)$$

Where K_6 is a positive scalar

$$\dot{V}_6 = \dot{V}_4 + \dot{V}_5 + e_6 \dot{e}_6$$

$$\dot{e}_6 = -K_6 e_6 = \frac{R_g}{L_g} i_{gq} + \omega i_{gd} - \frac{1}{L_g} E_q + \frac{1}{L_g} V_{gq} \quad (41)$$

We deduce E_{qref} the final backstepping control law is designed as:

$$E_{qref} = L_g(K_6 e_6 + \frac{R_g}{L_g} i_{gq} + \omega i_{gd} + \frac{1}{L_g} V_{gq}) \quad (42)$$

Finally we define from the backstepping control, the reference variables v_{dref} , v_{qref} E_{dref} and E_{qref} necessary for the control respectively of the PMSG and the AC/DC/AC converter, while requiring stability of the cascaded subsystems to ensure an asymptotic stability of the overall system. The Figure 1 represents the global nonlinear control scheme of a grid-connected wind turbine equipped with a PMSG and an AC/DC/AC converter, managed by a robust nonlinear control strategy called backstepping, which allows us to follow dynamic references and stabilize the system against disturbances.

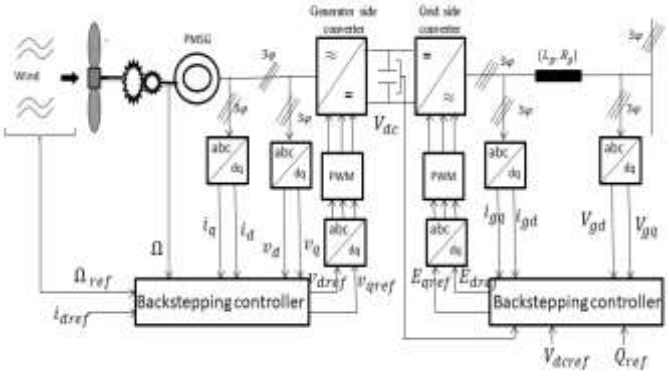

Fig. 1: Schematic representation of the backstepping control of the Turbine-PMSG and AC/DC/AC converter

6 Simulation Results and Discussion

6.1 Simulations Results

The adopted control is based on the Backstepping method applied to a GMSM, whose model is nonlinear and multivariable, the Table 1 shows the parameter values used to test the system through numerical simulation.

Table 1. The parameters of all systems

P	*4*
R_s	*0.6*[Ω]
L_d	*0.0014*[mH]
L_q	*0.0028*[mH]
φ_f	*0.2*[Web]
J	*0.02*[$N.mS^2/rad$]
f	*0.0014*
C_{pmax}	*0.39*
β	*2°*
ρ	*1.22 [kg /m3]*
λ_{opt}	*10*
G	*6*
R_g	*0.40*[Ω]
L_g	*0.025*[H]
C	*0.0042*[F]

6.2 Results and Discussion

The simulation results are obtained for the random wind speed closest to the evolution of the real wind are implemented in Figure 2, to adapt it to the slow dynamics of the system studied, And to prove control robustness Backstepping on the grid-connected wind energy conversion system. DC bus voltage regulation is shown in Figure 3. To control the voltage V_{dc}, the inverter injects surplus current into the network or vice versa, to discharge/charge the capacitor until (V_{dc}=V_{dcref}), at the same time as the inverter transmits the power used to the network. So, according to Figure 3, the DC bus voltage V_{dc} is well controlled at its 350V setpoint after a response time of 0.02s. After 0.02s, it is the permanent regime. Generally, the DC bus voltage $V_{dc}$is fixed, even in the presence of load variations and network conditions.The Figure 6 and Figure 7 show the results of (P, Q) control in the Park reference frame (d,q). The current signals in the Park frame, i_{gd} and i_{gq}, are presented about their references in Figure 4 and Figure 5. Through these currents, we can control the active power P and reactive power Q. In Figure 6 and Figure 7, we observe that the active power P injected by the inverter into the grid closely

follows the reference Pref. Consequently, the current i_{gd} perfectly tracks its reference i_{gdref}. The same applies to the current i_{gq}, which oscillates around its reference i_{gqref} and has an average value close to zero. The reactive power Q follows the reference Q_{ref}, which is set to zero, to maintain a unity power factor in the system. Figure 8 illustrates the phase difference between the current i_{ga} and the voltage V_{ga}on the grid-side converter, which is equal to zero. They also have the same frequency of 50Hz, which is the grid frequency.

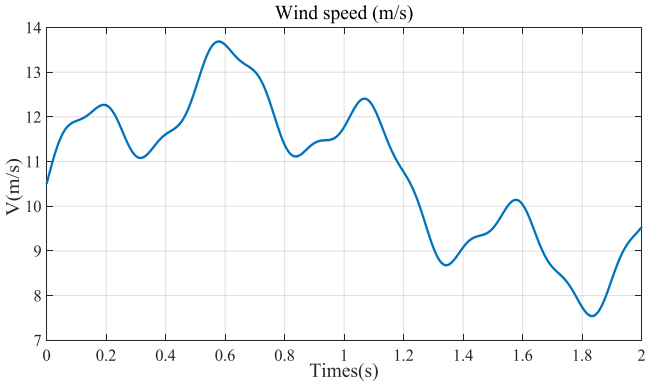

Fig. 2: Random wind speed profile

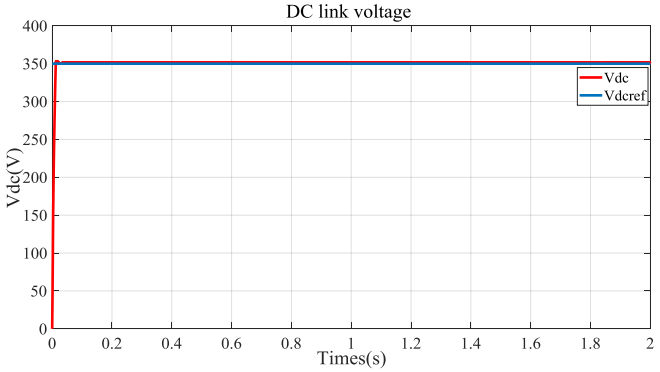

Fig. 3: The DC link voltage

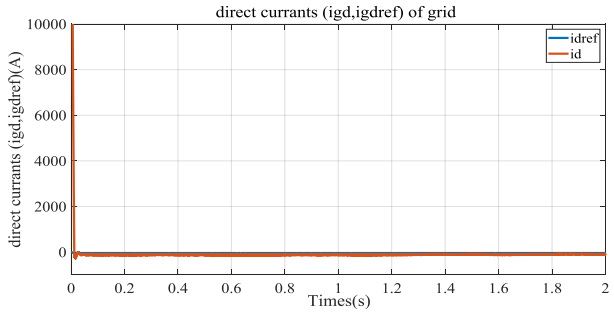

Fig. 4: The grid direct currants (i_{gd} i_{gdref})

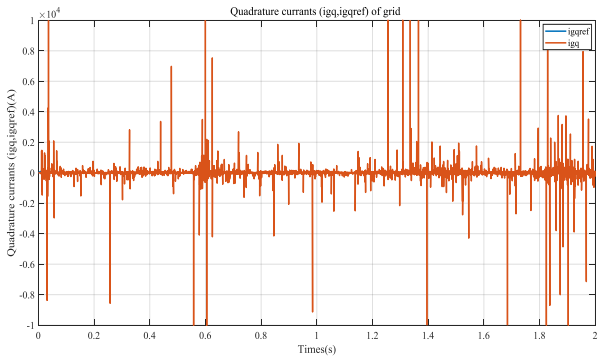

Fig. 5: The grid quadratur currants (i_{gq}, i_{gqref})

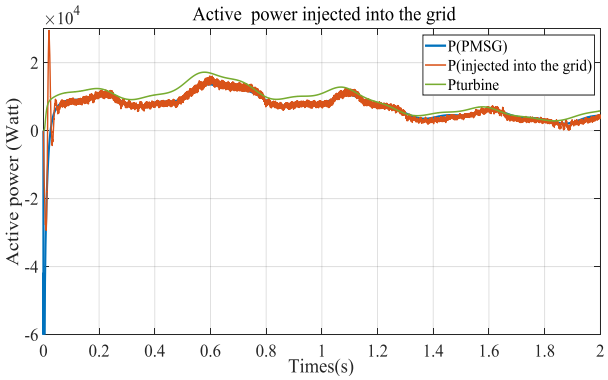

Fig. 6: The active power injected into the grid

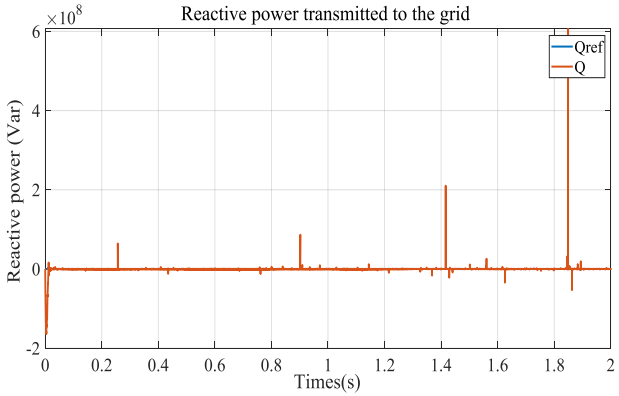

Fig. 7: The reactive power injected into the grid

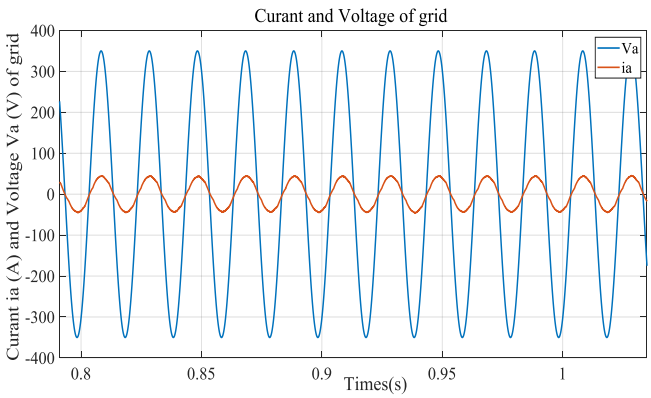

Fig. 8: The phase difference between the current i_ga and the voltage V_gaon the grid-side converter

The research work addressed in this study can be applied in the field of renewable energies and can even be extended and combined with other tools such as wavelets and artificial intelligence, as illustrated in references, [13], [14].

7 Conclusions

In our study, we thoroughly examined the use of backstepping control in managing a grid connected wind power generation system that utilizes a permanent magnet synchronous generator (PMSG) connected to the grid through an AC/DC/AC converter. We conducted simulations based on varying wind speeds to reflect real-world conditions. The results demonstrate the capability of the system to optimize power extraction, from wind sources maintain DC bus voltage, and manage the exchange of reactive and active power, with the grid effectively. The objective of this research was to develop a robust and efficient control scheme that can ensure stable operation, seamless grid synchronization, and optimal power transfer in grid connected wind power systems.

References:

[1] A. Drabyk, "Renewable Energy--Its Physics, Engineering, Environmental Impacts, Economics and Planning," *Journal of Environmental Quality,* vol. 30, p. 1098, 2001, https://doi.org/10.2134/jeq2001.3031098-ax.

[2] K. Ghedamsi, D. Aouzellag, and E. Berkouk, "Control of wind generator associated to a flywheel energy storage system," *Renewable Energy,* vol. 33, pp. 2145-2156, 2008, https://doi.org/10.1016/j.renene.2007.12.009.

[3] N. Harrabi, M. Souissi, A. Aitouche, and M. Chaabane, "Intelligent control of grid-connected AC–DC–AC converters for a WECS based on T–S fuzzy interconnected systems modelling," *IET Power Electronics,* vol. 11, pp. 1507-1518, 2018, https://doi.org/10.1049/iet-pel.2017.0174.

[4] A. Singh and O. Roy, "Performance analysis of a PMSM drive using PID controllers," *Electronics Information and Planning,* vol. 37, pp. 80-87, December 2010.

[5] M. A. Melnichenko, A. I. Gorkaviy, and M. A. Gorkaviy, "Combined control in the system with modal pi-regulator," in Current Problems and Ways of Industry Development: Equipment and Technologies, ed: Springer, 2021, pp. 507-517. (In Komsomolsk-on-Amur, Russia), https://doi.org/10.1007/978-3-030-69421-0_54.

[6] S. Rebouh, A. Kaddouri, R. Abdessemed, and A. Haddoun, "Nonlinear control by input-output linearization scheme for EV permanent magnet synchronous motor," in *2007 IEEE Vehicle Power and Propulsion Conference*, 2007, pp. 185-190. (In Arlington, TX, USA), DOI: 10.1109/VPPC.2007.4544122.

[7] M. A. Hamida, A. Glumineau, J. De Leon, and L. Loron, "Robust adaptive high order sliding-mode optimum controller for sensorless interior permanent magnet synchronous motors," *Mathematics and Computers in Simulation,* vol. 105, pp. 79-104, 2014, https://doi.org/10.1016/j.matcom.2014.05.006.

[8] Y. Chaou, S. Ziani, H. B. Achour, and A. Daoudia, "Nonlinear control of the permanent magnet synchronous motor PMSM using backstepping method," *WSEAS Transactions on Systems and Control,* vol. 17, pp. 56-61, 2022, https://doi.org/10.37394/23203.2022.17.7.

[9] C. Youssef, Z. Said, and D. Abdelkarim, "Backstepping Control of the Permanent Magnet Synchronous Generator (PMSG) Used in a Wind Power System," in *The International Conference on Artificial Intelligence and Smart Environment*, 2022, pp. 276-281. (In Errachidia, Morocco), DOI: 10.1007/978-3-031-26254-8_38.

[10] C. Youssef, Z. Said, and D. Abdelkarim, "Electric Vehicle Backstepping Controller Using Synchronous Machine," in *The International Conference on Artificial Intelligence and Smart Environment*, 2022, pp. 367-373. (In Errachidia, Morocco), DOI: 10.1007/978-3-031-26254-8_52.

[11] J. Wang, D. Bo, X. Ma, Y. Zhang, Z. Li, and Q. Miao, "Adaptive back-stepping control for a permanent magnet synchronous generator wind energy conversion system," *international journal of hydrogen energy,* vol. 44, pp. 3240-3249, 2019, https://doi.org/10.1016/j.ijhydene.2018.12.023.

[12] J. Zhou and Y. Wang, "Real-time nonlinear adaptive backstepping speed control for a PM synchronous motor," *Control Engineering Practice,* vol. 13, pp. 1259-1269, 2005, https://doi.org/10.1016/j.conengprac.2004.11.007.

[13] Q. Xu, T. Dragicevic, L. Xie, and F. Blaabjerg, "Artificial intelligence-based control design for reliable virtual synchronous generators," *IEEE Transactions on Power Electronics*, vol. 36, pp. 9453-9464, 2021, DOI: 10.1109/TPEL.2021.3050197.

[14] H. Yousuf, A. Y. Zainal, M. Alshurideh, and S. A. Salloum, "Artificial intelligence models in power system analysis," *in Artificial intelligence for sustainable development: Theory, practice and future applications*, ed: Springer, 2020, pp. 231-242, https://doi.org/10.1007/978-3-030-51920-9_12.

Contribution of Individual Authors to the Creation of a Scientific Article (Ghostwriting Policy)

- YOUSSEF CHAOU: Methodology, Software and Writing - original draft
- SAID ZIANI: Visualization and Validation
- HAFID BEN ACHOUR: Visualization
- ABDELKARIM DAOUDIA: Supervision
- YOUSSEF EL HASSOUANI: Supervision

Sources of Funding for Research Presented in a Scientific Article or Scientific Article Itself

No funding was received for conducting this study.

Conflict of Interest

The authors have no conflicts of interest to declare.